Impact strength of Friction Stir Weld-bonded joint

Bruno Figueira
bruno.figueira@tecnico.ulisboa.pt

Instituto Superior Técnico, Universidade de Lisboa, Portugal

May 2020

Abstract

The transport industry is constantly in search of new economically viable technological solutions aimed at reducing pollutant emissions and fuel consumption. One way to achieve these goals is to use lighter materials such as aluminium alloys. However, these materials have a reduced weldability, which leads to the search for new joining processes that aim to solve this problem. Friction Stir Welding (FSW) is a possible solution to achieve high quality joints without compromising significantly their mechanical properties when compared to the base material, for a butt joint configuration. However, when this technology is used in the overlap configuration, their properties are considerably reduced. In order to overcome this problem and improve the mechanical performance of these joints, a combination between FSW and adhesive is made. In this study, three different types of joints, using FSW, Adhesive Bonding (AB) and Friction Stir Weld-Bonding (FSWB), were produced. These joints were later studied in tensile and impact tests, to assess their mechanical performance at different loading rates. Numerical models were also developed in order to predict the mechanical behaviour of each joint under the previously studied loading. Hybrid joints showed significant improvements in comparison to the FSW joints when subjected to quasi-static loadings. Despite this, adhesive joints continue to perform better in general. In impact loadings, adhesive present on the hybrid joints significantly increases the capacity to absorb the energy from the impact in comparison to the FSW joints, changing the fracture mode of the joint.
Keywords: Friction Stir Welding, Hybrid joining, Friction Stir Weld-bonding, Lap joining, High strain rate, Numerical modelling

1. Introduction

Transport industry, especially automotive and aeronautical ones, have always searched for new cost-effective ways of increasing the efficiency of their products while keeping or improving their reliability. Over the past years, automotive and aircraft manufacturers are facing stricter norms and environmental regulations to limit greenhouse emissions and reduce the usage of fossil fuels. One way to achieve this can be by targeting the weight of the structure without compromising the structural integrity of the all system, which is leading makers to continuously search for lighter material solutions and manufacturing processes.

Friction Stir Weld-bonding (FSWB) is a promissing technology that aims to combine the advantages of both Friction Stir Welding (FSW) and Adhesive Bonding (AB).

2. Background

Friction stir welding (FSW) was invented in 1991 by Wayne Thomas, at The Welding Institute (TWI Ltd). It represented an important breakthrough in joining technologies in a sense that it became possible to produce high integrity joints in difficult or even non-weldable designated materials. Since there is no melting of material, mechanical properties of FSW are usually better when compared to fusion welding techniques.

FSW utilizes a tool composed by a non-consumable cylindrical shoulder with a plugged pin on the tip. The shoulder is responsible to create and keep the heat beneath it, whereas the pin function is to mix the material in the welding zone. Rotational and translational movement of this tool enables the joining of similar or dissimilar materials to be accomplished.

Plastic deformation and heat input involved in this process leads to a recrystallization of the base material and a micrographic analysis allows to distinguish 4 zones with different physical and mechanical properties [1]: base metal (BM), heat affected zone (HAZ), Thermo-mechanically affected zone and Stir zone (SZ). Size and properties of this zones are defined by the material flow and temperature distribution around the tool, which are influence mainly by the rotational speed, welding transverse speed, axial force and tool geometry [1].

FSW is a technology that is does not produce

harmful emissions, fully automated and capable of producing high quality weld seams and join dissimilar materials difficult to join through fusion welding without the appearance of hot cracking and porosity and excessive distortion and shrinkage of the work piece.

The intense investigation around FSW and results obtained from it has produced a fast spread of this technologies to various industries, with a special focus on the transportation industry, such as aerospace, railway and automotive industries [2]. Some concrete applications are present in the Delta II and IV, from Boeing, in the A380, from Embraer, in the Mercedes SL (R231), from Mercedes-Benz, and in the Honda Accord from Honda Motor Company.

Although FSW can be performed in a wide range of configurations, the typical geomeotries used are butt and lap joints. Butt joints tend to show tolerance problems which sometimes forces the use of lap joint. This joints present a great reduction in mechanical performance comparatively to the base material and so, hybridization of this process is seen as the option to overcome certain defects present in this type of joint, such as the hook defect. To accomplish this, adhesive can be added to this joint.

Adhesive bonding (AB) presents many advantages over the conventional mechanical fasteners, such as a more uniform stress distribution, which provides better load distributions, increase in fatigue life and weight savings [3]. Despite all this, adhesives are extremely sensitive to environmental attacks, substrate surface condition and load direction.

A combination between FSW and AB should overcome the downsides of each technique and produce a viable joining method. This innovative method is called Friction Stir Weld-bonding (FSWB). A detailed study of this joining method was conducted in [4], using AA6082-T6 as the substrate and Araldite 420 A/B as the adherent. From this study, it was concluded that surface treatment is crucial to obtain a strong bond between the adherent and the substrate, being phosphoric acid anodizing (PAA) prefered over sandblasting. Also, FSWB joints show an increase up to 60% in tensile strength when compared to FSW only joints, whereas in comparison to the AB joints mechanical performance of the FSWB is equal, at best.

An important aspect that has not been studied yet and will be focused in this research study is the behaviour of the FSWB under impact conditions. This is an important characteristic to take into account in the transport industry since the structures need to be dimensioned to protect the occupants in case of an impact occurence.

Study of the material properties at high strain rates can usually be done in Drop-Weight (DW) machines or in a Split Hopkinson Pressure Bar (SHPB) and, although these machines usually perform compression tests, some few modifications in the machine's structure are enough to allow tensile tests [5, 6]

3. Experimental procedure

3.1. Material properties

The base material used in this study was the 2 mm thick AA6082 aluminium alloy in T6 conditions. Mechanical properties of this alloy are presented in Tab.1. For the AB and hybrid joints, Araldite 420 A/B was the chosen adhesive.

3.2. FSW and hybrid joints manufacturing

FSW and hybrid single lap joints were manufactured with a 40 mm overlap, Fig.1 and Fig.2 respectively.

Figure 1: FSW joints cross section (not to scale).

Figure 2: Hybrid and AB joints cross section (not to scale).

The manufacturing process started by abrading the aluminium sheets to remove the oxide layer present on the surface. After degreasing the oxide free surface, sheets used to manufacture FSW joints are ready to be welded. For the hybrid joints, it is necessary an extra step to promote the adhesion between the substrate and the adhesive. To accomplish this, the AC-130 sol-gel from 3M was used.

Welds were manufactured with the ESAB® LEGIO 3UL numeric control machine. In the plunging and dwelling stages machine was position controlled, whereas for the rest of the welding process force control was implemented. The tool used is composed by a 16 mm diameter shoulder and 5 mm diameter cylindrical pin.

A robust clamping system was used not only to hold the sheets in place but also to prevent distortion and reduce residual stresses. For the hybrid joints, before positioning the top sheet and fasten the clamping system, adhesive is applied on top of the bottom sheet with a nozzle mixer. FSW process should be perform within 15 minutes after closing the overlap to prevent degradation of the adhesive properties.

Table 1: Mechanical properties of aluminium alloy AA6082-T6.

Density [$\mathrm{Kg/m^3}$]	Young's modulus [GPa]	Ultimate tensile strength [MPa]	Yield tensile strength [MPa]	Elongation at break [%]
2700	69	330	270	9.8

Tab.2 shows the process parameters used to manufacture the joints.

Table 2: Parameters used to manufacture FSW and Hybrid joints.

Parameters	Values
FSW control	Vertical Force (450 kgf)
Rotational direction	CW
Tilt angle [deg.]	0
Pin length [mm]	3
Plunge speed [mm/s]	0.1
Dwell time [s]	7 (FSW), 14 (Hyb)
Welding speed [mm/min]	200
Rotational speed [rpm]	1000
Plunge depth [mm]	3.1 (FSW), 3.2 (Hyb)

In order to the adhesive achieve its full strength, a curing time between 1 to 2 weeks was employed on the hybrid joints. After this specimens were cut according to Fig.3.

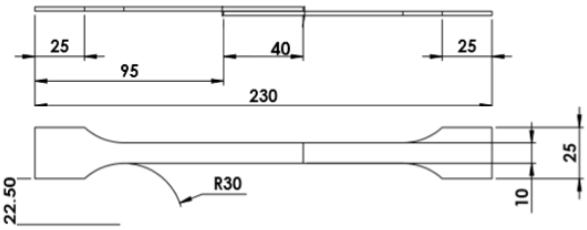

Figure 3: FSW,hybrid and AB 40 mm overlap specimens geometry.

3.3. AB joints manufacturing

AB single lap joints were manufactured with a 40 mm and a 12.5 mm overlap, Fig.2 and Fig.4 respectively. An adherent arm of 95 mm was used for both joints.

Figure 4: AB-12.5 mm overlap joint cross section (not to scale).

Surface preparation consisted in abrading, degreasing and application of an eletrochemical surface treatment - phosphoric acid anodizing - performed according to ASTM D3933-98 standard. This will help providing a good substrate/adhesive interfacial strength.

After this treatment, adhesive needs to be applied within 72 hours. Sheets were positioned in the mold and restrained with PTFE pins according to the overlap wanted. After closing the mold, curing of both adhesive joints was done in a hot plate hydraulic press, with time, temperature and pressure control. AB with 40 mm joints were manufactured also in a hot plate pneumatic press. Parameters used for both machines are present in Tab.3.

Table 3: Adhesive joints manufacturing parameters.

Parameters	Hydraulic press	Pneumatic press
Pressure [bar]	11	3.5
Temperature [°C]	120	130
Time [h;min]	1 h 45 min	2 h

AB with 40 mm and 12.5 mm overlap specimens were cut according to Fig.3 and Fig., respectively.

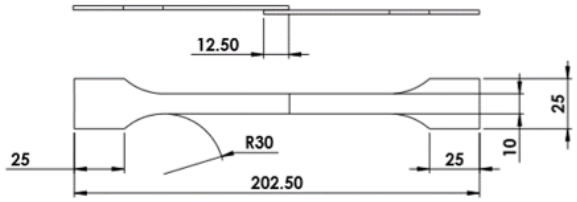

Figure 5: AB-12.5 mm overlap specimen geometry.

3.4. Microscopic analysis

A cross section sample was cut from the FSW and hybrid specimens and placed in a mold filled with an epoxy resin mixed with hardener. After a 24 hour rest, sanding and polishing of the sample's surface to be observed microscopically is performed with increasing grades of sandpaper and diamond compound polishers, respectively. Finally, a Keller's reagent etches the samples to contrast the different zones in the joint. Observation is done with the Olympus CK40M microscope.

3.5. Microhardness test

Samples previously used for the microscopic analysis were used again to characterize the mechanical and structural properties of the joints. These microhardness evaluations were performed by applying a load of 0.2 HV (1,961 N) during 10 sec along the mid-thickness lines of the top and bottom sheets of the joint. Each indentation was spaced by 0.3 mm and the testing machine used was the HMV-2 micro hardness tester.

3.6. Mechanical tests

3.6.1 Bulk dynamic test

To assess the mechanical behaviour of the adhesive an SHTB apparatus was used to perform bulk

adhesive tests. The used bars were made of titanium with a diameter of 16mm. The length of the incident and transmission bars are 5700mm and 2500mm, respectively. Strain gauges are placed within 2400mm and 400mm from the incident bar/specimen and transmission bar/specimen interfaces. The length of the striker is 1500mm and is propelled by a gas gun at 11m/s (pressure of 3bar). Specimens were subjected to a strain rate of 267 s^{-1} and geometry of the specimen used is detailed in Fig.6.

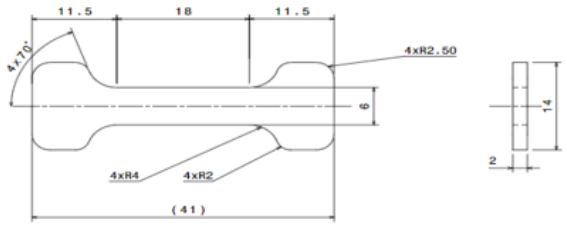

Figure 6: Adhesive bulk specimen geometry.

3.6.2 Quasi-static tests

Lap shear strength tests were performed for the different types of joints manufactured. Tests were performed using the INSTRON® 5566 testing machine, equipped with a load cell with a maximum capacity of 10 kN, at a displacement rate of 1 mm/min. For AB with 40 mm overlap, tests were also performed at 100 mm/min.

3.6.3 Impact tests

Impact behavior of the joints was assessed in a purpose made testing device. An electromagnetic actuator [7] was used to propel a striker bar. This mechanism uses a bank of capacitors (each with 6 mF) to store the energy needed and, once all the capacitors are ready, they will fire simultaneously to its respective coil, generating the pressure needed to accelerate the striker bar. The striker bar hits a transmission bar that slides on top of 3 guides. While one of the ends of the specimen is restrained, the other one is fixed with a bolt to the top of the transmission bar. This system allows the pulling of the specimen in only one direction, executing a tensile test at much higher speeds than the quasi-static ones. Specimen load and displacement data was acquired by a load cell and a displacement transducer, respectively Tests were performed for various velocities by changing the energy stored in each capacitor.

4. Results & discussion

4.1. Base Material characterization

Fig.8 compares the representative load displacement curves for the BM at displacement rates of 1 mm/min and 100 mm/min and with the grain on the longitudinal (LT) and long transverse (TL) directions. No significant differences in strength and

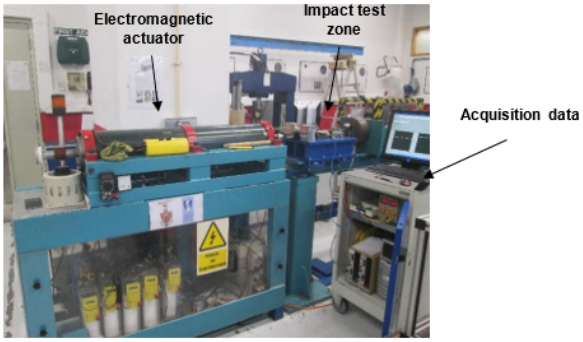

Figure 7: Impact test apparatus.

ductility were found between the two at the same displacement rates, meaning that grain direction doesn't not influence specimen's performance.

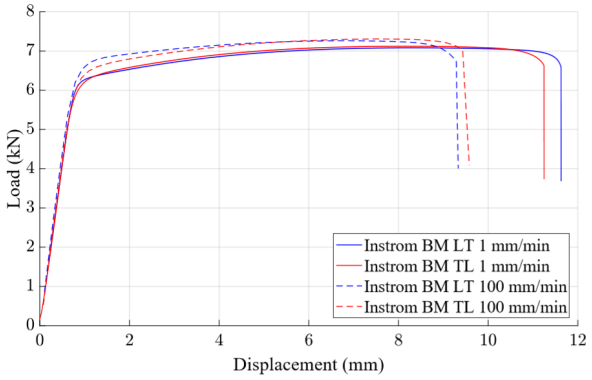

Figure 8: Adhesive bulk specimen geometry.

4.2. Adhesive mechanical characterization

Adhesive bulk tests obtained in the SHTB combined with previously results obtained at lower strain rates allowed to estimate the UTS values in a strain rate range up to the magnitude of the 10^2 s^{-1}, Fig.12.

From this tests, it was noticed that, although strengthening of the adhesive is increasing in an exponential trend with the increase of the strain rate, ductility is highest for lower strain rates and continuously decreases up until strain rates in the magnitude of the 10^{-2} s^{-1}, where trend inverts, and ductility starts to rise again.

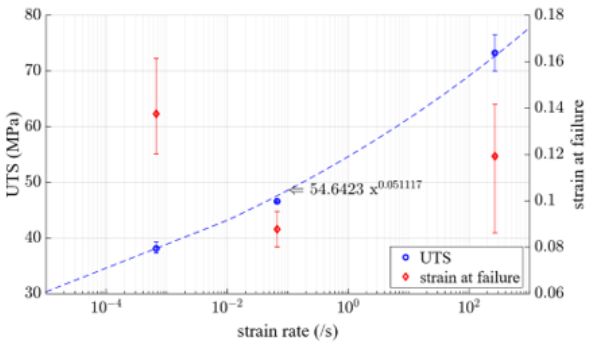

Figure 9: Adhesive bulk specimen geometry.

4.3. Microstructural evaluation

A representative macrostructure of the FSW process is shown in Fig.10, where it is possible to see the new zones that appear from this process. Two

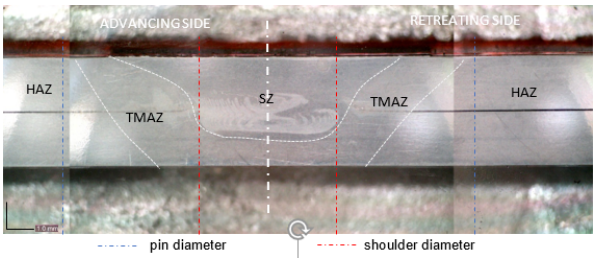

Figure 10: Representative macrostructure of AA6082-T6 FSW SLJ.

defects appear in the joint: in the advancing side (AS) hook defect is present, whereas in the retreating side (RS) the cold lap defect appears. These defects affect greatly the effective sheet thickness of the joints, seing a reduction from 2 to 1.5mm in the AS and from 2 to 0.8mm in the RS.

For the hybrid joints, although the defects are still present, they seem to be filled with adhesive, reinforcing these crack-like zones.

4.4. Microhardness profile

Microhardness measurements for both FSW and hybrid joints are presented in Fig.11 and Fig.Fig.12.

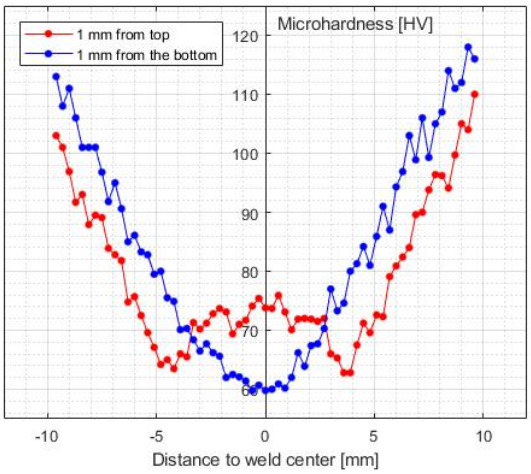

Figure 11: FSW-1 cross section microhardness.

A significant hardness decrease is seen in the HAZ and TMAZ, with some values even reaching about 50% of the base material (typical values around 110 HV), being the top sheet of the joint the most affected region and, consequently, the one with lower overall hardness values. This was expected since the thermal cycle is more intense on the shoulder zone, leading to smaller recrystalized grains. This difference between the overall hardness values is more evident on the hybrid joints

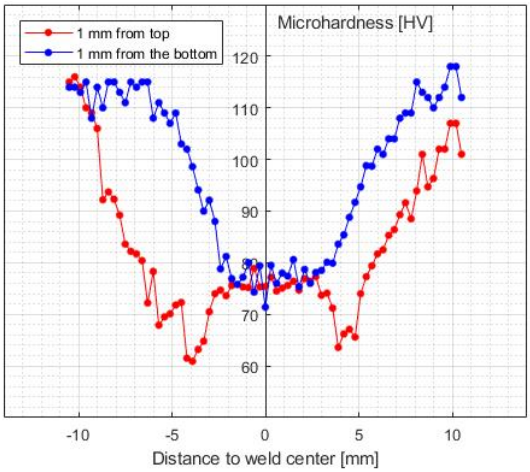

Figure 12: Hyb-3 cross section microhardness.

since there is an adhesive layer in between the upper and bottom sheets with a much lower thermal conductivity value, preventing most of the dissipation of heat from the top to the bottom sheet.

Although the lowest hardness values were noticed in the TMAZ on the AS, which also corresponds to the area of fracture zone, there is no significant difference in hardness between the AS and RS.

4.5. Single lap shear tests

Representative load displacement curves for the different type of joints are displayed in Fig.13, followed by Tab.4 with the respective values for average maximum load, maximum displacement and UTS.

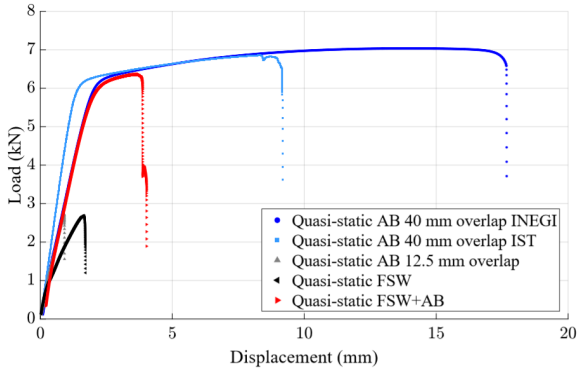

Figure 13: Representative load displacement curves of FSW, hybrid and adhesive bonded with 12.5 mm and 40 mm overlap joints.

AB 40mm overlap INEGI joints registered the highest strength and ductility, with fracture occurring in the substrate. Reducing the overlap from 40 to 12.5mm leads to a significantly decrease in both strength and ductility since overlap length cannot sustain as much damage as before. The AB manufactured at IST registered a 5% decrease in performance in comparison to the ones manufactures

Table 4: Characteristics of the lap shear strength tests of the different joints.

Joint	Max. load [kN]	Max. disp. [mm]	UTS [MPa]
FSW	$2.80^{+0.11}_{-0.11}$	$1.73^{+0.02}_{-0.02}$	$139.83^{+5.62}_{-5.62}$
FSW + AB	$6.24^{+0.12}_{-0.24}$	$3.55^{+0.43}_{-0.82}$	$311.88^{+6.16}_{-12.17}$
AB40mm IST	$6.71^{+0.14}_{-0.09}$	$7.07^{+2.10}_{-1.33}$	$335.60^{+7.13}_{-4.52}$
AB40mm INEGI	$7.09^{+0.03}_{-0.05}$	$16.99^{+1.15}_{-1.73}$	$354.49^{+1.41}_{-2.62}$
AB12.5mm	$2.60^{+0.13}_{-0.13}$	$0.86^{+0.10}_{-0.10}$	$129.87^{+6.30}_{-6.30}$

at INEGI, mainly due to the curing conditions and poorer surface treatment, leading also to a fracture through the adhesive. In the FSW joints fracture is originated in the hook defect which, consequently, leads to the low strength and ductility values obtained in the lap shear tests. Application of the adhesive layer on the hybrid joints attenuates this defect, reaching a increase in strength and ductility of 123% and 105% on average, respectively.

Joint efficiency was obtained by calculating the ratio between the remote stress of the joint and the ultimate tensile strength of the base material, Fig.14. Joint hybridization leads to an improvement of around 49% comparatively to the FSW joints, which corroborates the filled crack-like zones mentioned previously. All the 40 mm overlap adhesive joints had a performance superior to the hybrid ones, with the best manufacture AB joints even reaching a 102.4% joint efficiency. A 3% increase in efficiency when increasing the strain rate of the adhesive joint was noticed, which indicates a strain hardening on the adhesive part. The reduction in overlap from 40 to 12.5 mm resulted in a 65.5% performance decrease.

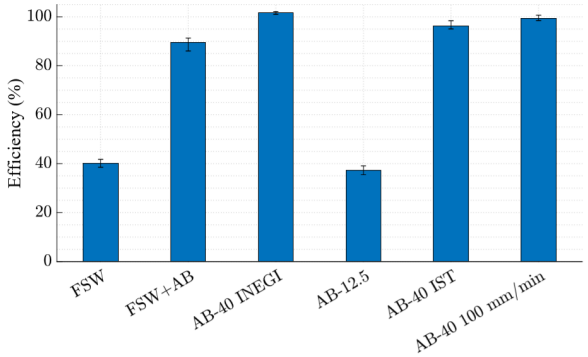

Figure 14: Efficiency of each joint type manufactured.

4.6. Impact tests

Representative load displacement curves for FSW and Hyb joints are displayed in Fig.15.

In the FSW, joint strength values reached a 32% increase while ductility increased 22%. This rate sensitivity in coherent with [8] may also indicate the strain rate dependency of the other zones, with different mechanical properties, in the centre of the joint. For the Hyb joints, only a 9% increase in joint strength is obtained. However, a 680% increase in ductility is noticed, which can be explained by the high ductility of the adhesive in use, and its ability to withstand impact loadings.This characteristic is extremely important since it determines the capability of the joint to absorb the energy of the impact.

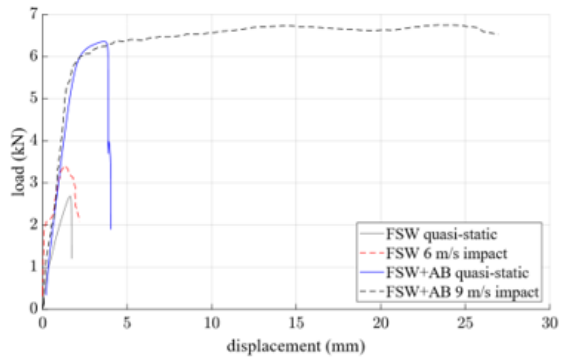

Figure 15: Representative load displacement curves for FSW and Hyb specimen at different displacement rates.

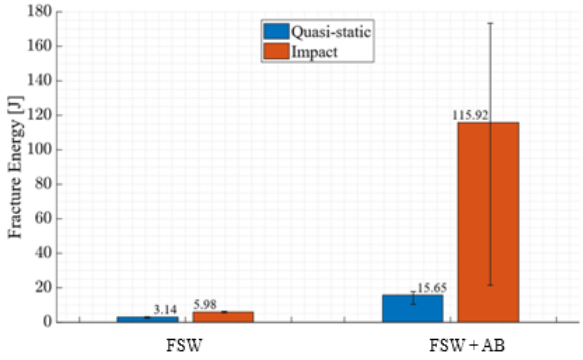

Figure 16: Fracture energy comparison between quasi-static and impact events.

In Fig.16, an estimative of the energy absorption is done by calculating the area beneath the load-displacement curve. An increase by 400% and by 1840% in the energy absorbed by the hybrid joints when comparing to the FSW only joints is noticed. However, scatter in the hybrid joints at impact experiments is significantly higher then the FSW joints. This seems to occur because these joints present 2 different types of fractures whether they are under the 9 m/s impact's velocity or above. If under, fracture starts in the adhesive, leading to a final fracture through the hook defect, whereas if the opposite occurs adhesive can absorb as much energy as possible until the joint fracture to the new weakest point, which is the aluminium substrate, Fig.17.

5. Numerical analysis

A 3D FEM model was created for each joint using the ABAQUS® software package. Dynamic

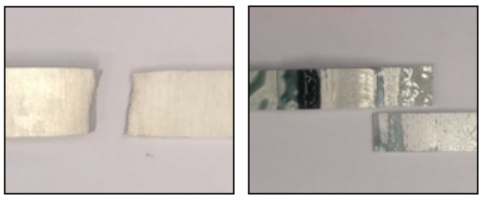

(a) Above 9 m/s. **(b)** Below 9 m/s.

Figure 17: Type of fractures in the hybrid joints.

explicit analyses were performed for both quasi-static and impact events. To model the elastic behaviour of the aluminium, Young modulus and Poisson's ratio was given. As for the plastic properties, an isotropic hardening law (Voce law) was used, along side a ductile damage criterion (GTN model) to more accurately predict failure of the aluminium by taking into consideration the decrease in stiffness and strength of the metal due to porosity (damage variable). Mechanical properties of the different aluminium zones were assessed with the aid of DIC measurements in [4] and modelling of these zones was done based on the microscopic and microhardness measurements, Fig.18. Hook defect was also represented in the advancing side.

For the adhesive component, cohesive zone modeling (CZM) was used to model its behaviour. This method uses the relationship between peel and shear stress to stimulate the elastic behaviour and subsequent softening due to degradation of the material properties. Mechanical properties at quasi-static rate were assessed both in tension and shear using DIC measurements in [4], whereas at impact rate were obtained using a SHTB in the present work.

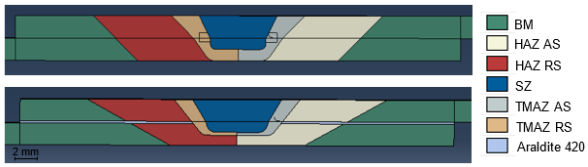

Figure 18: Representation of the different zones of the FSW and Hybrid numerical models, respectively.

Two element types were used: continuum three-dimensional 8-node element (C3D8R) for the aluminium zones and 8-node three-dimensional cohesive element (COH3D8) for the adhesive. To reproduce the experimental conditions, bottom sheet was restrained and a displacement or a predefined velocity field was set on the top plate, depending on if the simulation was for quasi-static or impact events, respectively. An additional symmetry condition along the loading axis was also defined, to reduced computational effort and, for the impact simulations, an extra mass was added on the top plate to simulate the striker's mass.

5.1. AB-12.5 SLJ

Fig.19 shows a comparison between the experimental and numerical results obtained for the AB joints with a 12.5 mm overlap.

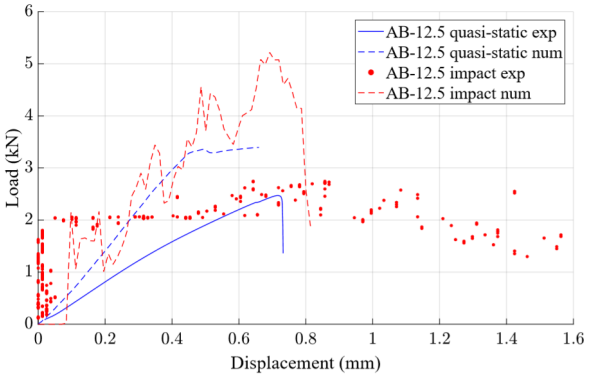

Figure 19: Experimental and numerical load displacement curves of the AB-12.5 specimens.

For the quasi-static experiments, significant stiffness difference between experimental and numeric is noticeable since machine compliance is not taken into account. Also, joint strength in the numerical model is overpredicted and there is plasticization of the joint, whereas in the experimental cases joints deform almost only elastic. This can be explained not only as a result of the simulation in considering perfect adhesion between the substrate and the adhesive, which may not be completely true in this case and leads to a premature failure, but also due the slipping that occurred in these tests, as mentioned before.

For the impact experiments, significant noise is present in the experimental curve, which makes it difficult to establish a comparison between experimental and numerical impact tests, being a point to improve. However, it is possible to see a significant difference in strength and ductility, which might indicate that damage model of the adhesive might not be adequate for this strain rate magnitude and should be reviewed.

5.2. AB-40 SLJ

A comparison between the experimental and numerical results obtained for the AB joints with a 40 mm overlap is shown in Fig.20. Numerical curves present a stiffer joint behaviour since displacement values are measured on the cross head LVDT of the machine.

These joints were modelled using a new isotropic law (Voce law) since in the present study mechanical properties of the BM were assessed. In the quasi-static experiments, while strength was accurately predicted, ductility of the joint was underpredicted. Ductility of the joint might have been higher experimentally due to the clamping system slipping.

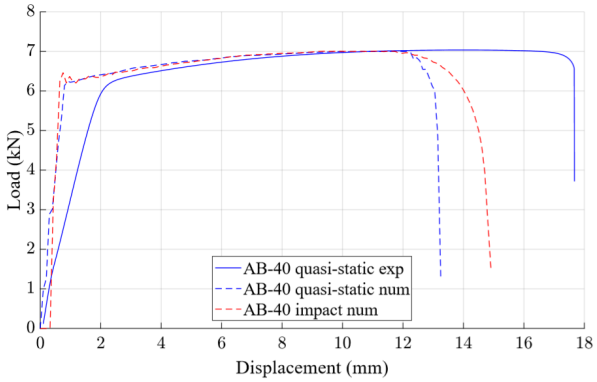

Figure 20: Experimental and numerical load displacement curves of the AB-40 specimens.

For the impact tests, despite a comparison between experimental and numeric could not be made, it is possible to notice in the latter that the ductility of this joint increases with the increase in the strain rate, which was expected due the high ductility characteristic of this type of adhesive.

Failure mode was well predicted, with the joint failing in the substrate, away from the overlap

5.3. FSW SLJ

A comparison between the experimental and numerical results obtained for the FSW joints is shown in Fig.21. Stiffness in simulation is significantly higher than experimentally due to the influence that the slipping of the clamping system has in the results.

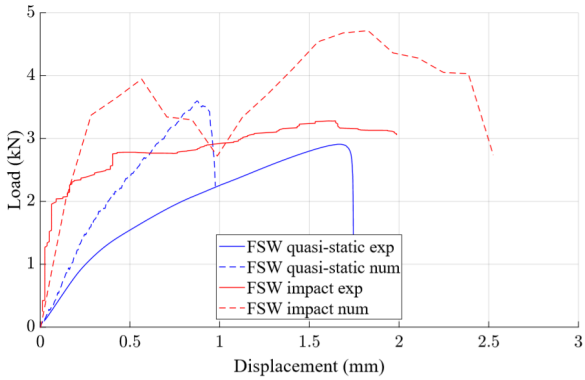

Figure 21: Experimental and numerical load displacement curves of the FSW specimens.

In the quasi-static, strength in the numerical model is overpredicted, whereas for ductility the opposite happens. This can occur due to lack of representation of the residual stresses resultant from the welding process. Also, in the numerical model change in the material properties between zones occurs abruptly, leading to stress gradients that push the fracture of the joint to be in these boundary changes.

For the impact tests, significant noise is present in the experimental curve which makes it hard to compare both curves. Despite this, an overprediction and underprediction of the strength and ductility of the joint, respectively, may indicate that this material can be rate sensitive around the range of strains tested.

Fracture in this case was also well predicted, being initiated in the hook defect

5.4. Hyb SLJ

A comparison between the experimental and numerical results obtained for the hybrid joints is shown in Fig.22

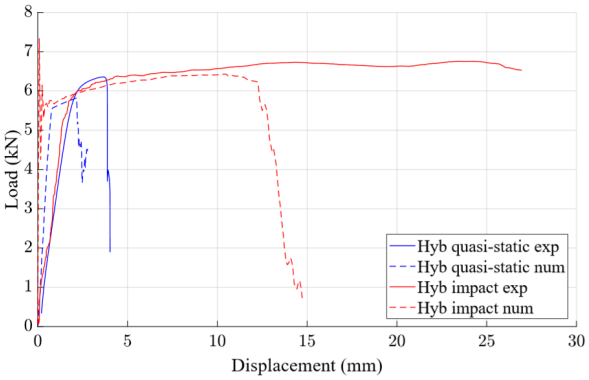

Figure 22: Experimental and numerical load displacement curves of the hybrid specimens.

Quasi-static results show that, although both strength and ductility of the numerical model is lower comparatively to the experimental one, type of failure is the same: it starts with the majority of the adhesive failing simultaneously, shortly followed by the failure of the aluminium substrate in the transition zone between HAZ and TMAZ.

When strain rate is increased, strength prediction of the joint starts to get close from the experimental, even though change in strength between the different rates is not significative. For velocities up to 6 m/s, joint failure is similar to the quasi-static failure, with the adhesive failing first and the aluminium failing shortly after, whereas for velocities above 9 m/s failure of the joint is similar to the adhesive bonded joint, which occurs in the substrate, away from the overlap. This may indicate that a transition in the adhesive behaviour occurs around these velocities. Ductility in this case is underpredicted, which might indicate that a study to characterize the adhesive at high strain rates should be done in the future, similarly to the one done in [4] for quasi-static.

When comparing hybrid and FSW simulations, similar conclusion to the experimental tests can be withdrawn, Fig.23. Adhesive addition to the FSW process substantially improves strength and ductility of the joint, and the effect of the hook defect, which is the main cause of premature failure of the FSW joints, starts to get less evident.

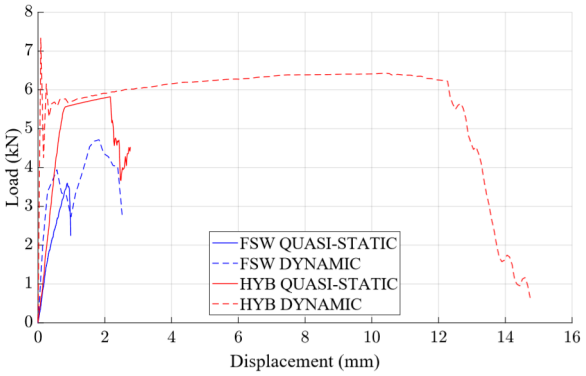

Figure 23: Experimental and numerical load displacement curves of the hybrid specimens.

6. Conclusions

At quasi-static loadings, hybrid joints performed constantly better than the FSW only joints, with an average joint efficiency of 89.5% comparatively to the 40.1% from the FSW ones. Although both joints suffer recrystallization of the base material, the nonexistence of free overlap area due to the adhesive layer, observed in the microscopy analysis, contributed significantly for this increase in performance. Despite this improvement, static mechanical performance of hybrid joints is still short when compared to the AB joints with a 40 mm overlap, with the best performing joint achieving a 102.4% joint efficiency. Reducing the overlap of the AB joints resulted in a decrease in performance of 65.5%.

At impact loading, hybrid joints showed their capability to absorb the energy from the impact, increasing by 680% in ductility. When compared to FSW joints, hybrid fracture energy was 1840% higher. For this to occur, a good surface treatment is pivotal to guarantee a strong bond between adhesive and substrate. It was also noticed two types of fracture for the hybrid joints depending on the impact's velocity.

In general accuracy of the models was not achieved. In order to increase accuracy of these models, aluminium damage model and hardening material laws for the HAZ, TMAZ and SZ zones should be reviewed since they were based from the literature. The new parameters used for the isotropic hardening law (Voce law) shown a good correlation for the base material, predicting accurately the base material strength.

References

[1] Rajiv S Mishra and ZY Ma. Friction stir welding and processing. *Materials science and engineering: R: reports*, 50(1-2):1–78, 2005.

[2] VM Magalhães, C Leitão, and DM Rodrigues. Friction stir welding industrialisation and research status. *Science and Technology of Welding and Joining*, 23(5):400–409, 2018.

[3] Lucas FM Da Silva, Andreas Öchsner, and Robert D Adams. *Handbook of adhesion technology*. Springer Science & Business Media, 2018.

[4] D. F. O. Braga. *Innovative structural joining for lightweight design*. MIT-Portugal, 2018.

[5] PH Mott, JN Twigg, DF Roland, HS Schrader, JA Pathak, and CM Roland. High-speed tensile test instrument. *Review of scientific instruments*, 78(4):045105, 2007.

[6] GH Staab and AMOS Gilat. A direct-tension split hopkinson bar for high strain-rate testing. *Experimental mechanics*, 31(3):232–235, 1991.

[7] CMA Silva, PAR Rosa, and PAF Martins. An innovative electromagnetic compressive split hopkinson bar. *International Journal of Mechanics and Materials in Design*, 5(3):281–288, 2009.

[8] Xuanzhen Chen, Yong Peng, Shan Peng, Song Yao, Chao Chen, and Ping Xu. Flow and fracture behavior of aluminum alloy 6082-t6 at different tensile strain rates and triaxialities. *PloS one*, 12(7), 2017.